Strength Predictions of Pile Caps by a Strut-and-Tie Model Approach

JungWoong Park, Daniel Kuchma, and Rafael Souza

JungWoong Park, Daniel Kuchma, and Rafael Souze

Address:

Department of Civil and Environmental Engineering,

University of Illinois at Urbana-Champaign.

2114 Newmark Laboratory, 205 N. Mathews Ave., Urbana, IL, 61801, USA.

Corresponding author: Daniel Kuchma

Address:

Department of Civil and Environmental Engineering,

University of Illinois at Urbana-Champaign.

2106 Newmark Laboratory, 205 N. Mathews Ave., Urbana, IL, 61801, USA.

(217)-333-1571 (Phone)

(217)-333-9464 (Fax)

kuchma@uiuc.edu

Abstract

In this paper, a strut-and-tie model approach is presented for calculating the strength of reinforced concrete pile caps. The proposed method employs constitutive laws for cracked reinforced concrete and considers strain compatibility. This method is used to calculate the load carrying capacity of 116 pile caps that have been tested to failure in structural research laboratories. This method is illustrated to provide more accurate estimates of behavior and capacity than the special provisions for slabs and footings of 1999 American Concrete Institute (ACI) code, the pile cap provisions in the 2002 CRSI Design Handbook, and the strut-and-tie model provisions in either 2005 ACI code or the 2004 Canadian Standards Association (CSA) A23.3. The comparison shows that the proposed method consistently well predicts the strengths of pile caps with shear span-to-depth ratios ranging from 0.49 to 1.8 and concrete strengths less than 41 MPa. The proposed approach provides valuable insight into the design and behavior of pile caps.

Key words: strut-and-tie model, pile caps, footings, failure strength, shear strength

INTRODUCTION

The traditional design procedure for pile caps is the same sectional approach as that typically used for the design of two-way slabs and spread footings in which the depth is selected to provide adequate shear strength from concrete alone and the required amount of longitudinal reinforcement is calculated using the engineering beam theory assumption that plane sections remain plane. However, and as illustrated by simple elastic analyses, pile caps are three-dimensional D(Discontinuity) Regions in which there is a complex variation in straining not adequately captured by sectional approaches. A new design procedure for all D-Regions, including pile caps, has recently been introduced into North American design practice (Canadian Standards Association (CSA) 1984, the American Association of State Highway and Transportation Officials (AASHTO) 1994, American Concrete Institute (ACI) 2002). This procedure is based on a strut-and-tie approach in which an idealized load resisting truss is designed to carry the imposed loads through the discontinuity region to its supports. For the typically stocky pile cap, such as the four-pile cap shown in Fig. 1, this consists of compressive concrete struts that run between the column and the piles and steel reinforcement ties that extend between piles.

The strut-and-tie approach is a conceptually simple and generally regarded as an appropriate approach for the design of all D-Regions. To enable its use in practice, it was necessary to develop specific rules for defining geometry and stress limits in struts and ties that have been incorporated into codes of practice. These rules and limits were principally derived from tests on planar structures and they are substantially different for the two predominant strut-and-tie design provisions in North America, those being the “Design of Concrete Structures” by the Canadian Standards Association (CSA Committee A23.3 2004) and Appendix A “Strut-and-Tie Models” of the “Building Code Requirements for Structural Concrete” of the American Concrete Institute (ACI Committee 318 2005). An evaluation of the applicability of these strut-and-tie provisions to pile caps should be made using available experimental test data. In addition, it would be useful to assess if the design of pile caps would benefit from any additional specific rules or guidelines in order to ensure a safe and effective design.

This paper presents an examination of existing design methods for pile caps as well as a new strut-and-tie approach for calculating the capacity of pile caps. This new approach utilizes constitutive laws for cracked reinforced concrete and considers both strain compatibility and equilibrium. To validate the proposed method, it is also used to calculate the strength of 116 pile caps with concrete strengths less than 41 MPa. These strengths are also compared with those calculated using the special provisions for slabs and footings of ACI 318-99 (ACI Committee 318 1999), CRSI Design Handbook 2002 (CRSI 2002), the strut-and-tie model provisions used in ACI 318-05 (ACI Committee 318 2005) and the Canadian Standards Association (CSA Committee A23.3 2004), and the strut-and-tie model approach presented by Adebar and Zhou (1996).

EXISTING PILE CAP DESIGN METHODS

This section provides a brief discussion of the aforementioned provisions and guidelines that are used in North American practice for the design of pile caps.

ACI 318-99 and CSRI Handbook suggest that pile caps be designed using the same sectional design approaches as those for slender footings supported on soil. This requires a design for flexure at the face of columns as well as one and two-way shear checks. The CSRI Handbook provides an additional relationship for evaluating $\boldsymbol{V_c}$ when the shear span is less than one-half the depth of the member, $w < d/2$, as presented in eq. [1] where $\boldsymbol{c}$ is the dimension of a square column. These procedures are the most commonly used in North American design practice.

[1] $$V_c = \left(\frac{d}{w}\right)\left(1+\frac{d}{c}\right)\left(0.33\sqrt{f_c'}\right)b_s d \quad \text{(mm, N)}$$

where the shear section perimeter is $b_s = 4c$.

Appendix A of ACI 318-05 and the Canadian Standards Association provide provisions for the design of all D(Discontinuity)-Regions in structural concrete, including pile caps. These provisions include dimensioning rules as well as stress limits for evaluating the capacity of struts, nodes, and the anchorage region of ties. They principally differ in the stress limits for struts. In ACI 318-05, the compressive stress for the type of bottle shaped struts that occur in pile caps would be $0.51 f_c'$. The stress limit in struts by the CSA strut-and-tie provisions are a function of the angle of the strut relative to the longitudinal axis, with the effect that the stress limit in 30, 45 and 60 degree struts with the assumption of tie strain $\varepsilon_s = 0.002$ would be 0.31, 0.55, and 0.73 f_c', respectively. The strut-and-tie provisions in these code specifications have only had limited use in design practice.

Based on an analytical and experimental study of compression struts confined by plain concrete, Adebar and Zhou (1993) concluded that the design of pile caps should include a check on bearing strength that is a function of the amount of confinement and the aspect ratio of the diagonal struts. Adebar and Zhou (1996) provided the following equations for the maximum allowable bearing stress in nodal zones:

[2; 3; 4] $$f_b \le 0.6 f_c' + 6\alpha\beta\sqrt{f_c'}\,; \quad \alpha = \frac{1}{3}\left(\sqrt{A_2/A_1} - 1\right) \le 1.0\,; \quad \beta = \frac{1}{3}\left(\frac{h_s}{b_s} - 1\right) \le 1.0$$

The parameters α and β account for the confinement of the compression strut and the geometry of the diagonal strut. The ratio A_2/A_1 in eq. [3] is identical to that used in the ACI code for calculating the bearing strength. The ratio h_s/b_s is the aspect ratio (height-to-width) of the strut. Adebar and Zhou suggested that the check described above is added to the traditional section force approach for pile cap design.

The calculated strengths by these provisions and design guidelines are compared against the test database following the presentation of the authors proposed strut-and-tie method and this test database.

A THREE-DIMENSIONAL STRUT-AND-TIE MODEL APPROACH

To further evaluate the effectiveness of a strut-and-tie design approach for pile caps and to identify means of improving design provisions, a methodology for evaluating the capacity of pile caps was developed that considers strain compatibility and uses non-linear constitutive relationship for evaluating the strength of struts. In this procedure, the three-dimensional strut-and-tie model shown in Fig. 1 was used for the idealized load resisting truss in a four-pile cap. This model is used for all pile caps examined in this paper. The shear span-to-depth ratio of most test specimens selected in this study is less than one. Since the mode of failure is not known for all test specimens, the proposed model considers the possibility of crushing of the compression zone at the base of the column and yielding of the longitudinal reinforcement (ties). For all truss models used in this study, the angle between longitudinal ties and diagonal struts is greater than 25 degrees; satisfying the ACI 318-05 limit. The details of the proposed strut-and-tie approach are now presented.

Effective depth of concrete strut

The effective strut width is assumed based on the available concrete area and the anchorage conditions of the strut. The effective area of diagonal strut at the top node is taken as

[5] $$A_d = \frac{c}{\sqrt{2}}\left(\frac{c}{\sqrt{2}}\cos\theta_z + kd\sin\theta_z\right)$$

where c is the thickness of the square column and k is derived from the bending theory for a single reinforced section as follows

[6] $$k = \sqrt{(n\rho)^2 + 2n\rho} - n\rho$$

and where n is the ratio of steel to concrete elastic moduli with E_c taken as follows (Martinez 1982)

[7] $$\boldsymbol{E_c} = \begin{cases} 4730\sqrt{\boldsymbol{f_c'}} & \text{for } \boldsymbol{f_c'} \le 21\,\boldsymbol{MPa} \\ 3320\sqrt{\boldsymbol{f_c'}} + 6900 & \text{for } \boldsymbol{f_c'} > 21\,\boldsymbol{MPa} \end{cases}$$

The inclination angles between the diagonal struts and x-, y-, and z-axis are expressed as θ_x, θ_y, and θ_z respectively as shown in Fig. 1. These angles represent the direction cosines of a diagonal strut. The effective area of a diagonal strut at the bottom node is taken as

[8] $$A_d = \frac{\pi}{4} d_p \left[d_p \cos\theta_z + 2(h-d)\sin\theta_z \right]$$

where d_p is pile diameter and h is overall height of the pile cap. The effective area of diagonal strut is taken as the smaller of eqs. [5] and [8]. The effective depth of a horizontal strut is taken as $h/4$ based on the suggestion of Paulay and Priestley (1992) on the depth of the flexural compression zone of the elastic column as follows

[9] $$w_c = \left(0.25 + 0.85 \frac{N}{A_g f_c'} \right) h_c$$

Force equilibrium

The strut-and-tie model shown in Fig. 1 is statically determinate and thus member forces can be calculated from the equilibrium equations only as given below:

[10] $$F_d = \frac{P}{4\cos\theta_y}$$

[11] $$F_x = F_d \cos\theta_x$$

[12] $$F_y = F_d \cos\theta_y$$

where P is column load; F_d is the compressive forces in the diagonal strut; F_x and F_y are respectively the member forces in the x- and y-axis horizontal struts and ties. Since the strut-and-tie method is a full member design procedure; flexure and shear are not explicitly considered.

Constitutive laws

Cracked reinforced concrete can be treated as an orthotropic material with its principal axes corresponding to the directions of the principal average tensile and compressive strains. Cracked concrete subjected to high tensile strains in the direction normal to the compression is observed to be softer than concrete in a standard cylinder test (Hsu and Zhang 1997, Vecchio and Collins 1982, 1986, 1993). This phenomenon of strength and stiffness reduction is commonly referred to as compression softening. Applying this softening effect to the strut-and-tie model, it is recognized that the tensile straining perpendicular to the compressive strut will reduce the capacity of the concrete strut to resist compressive stresses. Multiple compression softening models were used in this study to investigate the sensitively of the results to the selected model. All models were found to provide similarly good results as will be illustrated later in the paper. The compression softening model proposed by Hsu and Zhang (1997) was selected for the base comparisons and is now described, but it has been illustrated by the authors in a earlier paper (Park and Kuchma 2006) that different compression softening models can be similarly used. The stress of concrete strut is determined from the following equations proposed by Hsu and Zhang.

[13] $$\sigma_d = \xi f_c' \left[2\left(\frac{\varepsilon_d}{\xi\varepsilon_0}\right) - \left(\frac{\varepsilon_d}{\xi\varepsilon_0}\right)^2 \right] \quad \text{for } \frac{\varepsilon_d}{\xi\varepsilon_0} \le 1$$

[14] $$\sigma_d = \xi f_c' \left[1 - \left(\frac{\varepsilon_d / (\xi\varepsilon_0) - 1}{2/\xi - 1}\right)^2 \right] \quad \text{for } \frac{\varepsilon_d}{\xi\varepsilon_0} > 1$$

$$\xi = \frac{5.8}{\sqrt{f_c'}} \frac{1}{\sqrt{1+400\varepsilon_r}} \le \frac{0.9}{\sqrt{1+400\varepsilon_r}} \tag*{[15]}$$

where ε_0 is a concrete cylinder strain corresponding to the cylinder strength f_c', which can be defined approximately as (Foster and Gilbert 1996)

$$\varepsilon_0 = 0.002 + 0.001\left(\frac{f_c' - 20}{80}\right) \quad \text{for} \quad 20 \le f_c' \le 100 \quad \text{MPa} \tag*{[16]}$$

The response of the ties is based on the linear elastic perfectly plastic assumption.

$$F_{st} = E_s A_{st} \varepsilon_{st} \le F_{st} \tag*{[17]}$$

where A_{st} and F_{st} are the area and yielding force of horizontal steel tie in the x- or y-axes.

The proposed method considers a tension stiffening effect for evaluating the force and strain in steel ties. Vecchio and Collins (1986) suggested the following relationship for evaluating the average tensile stress in cracked concrete:

$$f_{ct} = \frac{f_{cr}}{1+\sqrt{200\varepsilon_r}} \tag*{[18]}$$

Taking f_{cr} as $0.33\sqrt{f_c'}$ and ε_r as 0.002, the tension force resisted by concrete tie is given by

$$F_{ct} = 0.20\sqrt{f_c'} A_{ct} \tag*{[19]}$$

where A_{ct} is the effective area of concrete tie which is taken as

$$A_{ct} = \frac{d}{4}\left(\frac{l_e}{2} + \frac{d_p}{2}\right) \tag*{[20]}$$

where l_e is the pile spacing.

Compatibility relations

The strain compatibility relation used in this study is the sum of normal strain in two perpendicular directions which is an invariant:

[21] $$\varepsilon_h + \varepsilon_v = \varepsilon_r + \varepsilon_d$$

where ε_d is the compressive strain in a diagonal strut and ε_r is a tensile strain in the direction perpendicular to the strut axis. Since horizontal and vertical web reinforcements were not available from test data, ε_h and ε_v are conservatively taken as 0.002 in eq. [21].

COMPARISON WITH TEST RESULTS

Existing test data

Blevot and Fremy (1967) tested 59 four-pile caps. The majority of the four-pile caps were approximately half-scale specimens, and eight of them were full-scale with 750-1000 mm overall heights. Since one of main objectives of this work was to verify a truss analogy method, they used different reinforcement details including no main reinforcement, and either uniformly distributed or bunched reinforcement between piles. Clarke (1973) tested 15 square four-pile caps with overall heights of 450 mm, all approximately half-scale. Two specimens had diagonal main reinforcement, three had main reinforcement bunched over the piles, and the remaining ten had uniformly distributed main reinforcement. The main variables in this study were pile spacing, reinforcement layout, and anchorage type. He reported that the first cracks formed on the centerlines of the vertical faces, and these cracks progressed rapidly upwards forming a cruciform pattern, and finally each cap split into four blocks. Such observations point strongly to a bending failure mode developing. However, though Clarke contended that the majority of the caps failed in shear, the authors agree with Bloodworth, Jackson, and Lee (2003) that many of these failure modes may be more accurately described as combined bending and shear failure. Sabnis and Gogate (1984) tested nine small-scale four-pile caps with 152 mm overall heights, of which one was unreinforced. They studied how the quantity of uniformly distributed longitudinal reinforcement influences the shear capacity of deep pile caps. They reported that cracking of the four outer faces was about the same in all the specimens and are indicative of combinations of deep beam failure with very steep shear cracks and punching shear failures of slabs. They also observed that some of this cracking may be prevented by the use of horizontal reinforcement on the vertical faces of the caps; this reinforcement is only of secondary benefit and might not substantially enhance the strength of the pile cap. Adebar, Kuchma, and Collins (1990) tested six full-scale pile caps to study the performance of the strut-and-model for pile cap design. Four of their tests were on diamond-shaped caps, one was on a cruciform-shaped cap, and one was on a rectangular six-pile cap. The test results demonstrated that the strain distributions are highly nonlinear both prior to cracking and after cracking. They reported that the failure occurs after a compression strut split longitudinally due to the transverse tension caused by spreading of the compressive stresses and that the maximum bearing stress is a good indicator of the likelihood of a strut splitting failure. From the pile caps they tested, the maximum bearing stress at failure had a lower limit of about $1.1f_c'$. They concluded that the strut-and-tie models accurately represent the behavior of deep pile caps and correctly suggest that the load at which a lightly reinforced pile cap fails in two-way shear depends on the quantity of longitudinal reinforcement. Suzuki, Otsuki, and Tsubana (1998, 1999), Suzuki, Otsuki, and Tsuchiya (2000), and Suzuki and Otsuki (2002) tested 94 four-pile caps with the reinforcement bunched over the piles or distributed in a uniform grid. The main variables investigated in tests were the influence of edge distance, bar arrangement, taper, and concrete strength on the failure mode and the ultimate strength. They reported that it was experimentally observed that the ultimate strength of the pile caps with a uniform grid arrangement was lower than that of pile caps with an equivalent amount of reinforcement concentrate (bunched) between the pile bearings. Though pile caps may be designed to any shape depending on the pile arrangement, rectangular four-pile caps previously tested were only chosen for examination in this study. Therefore, the 116 pile cap specimens tested by Clarke (1973), and Suzuki, Otsuki, and Tsubata (1998, 1999), Suzuki, Otsuki, and Tsuchiya (2000), Suzuki and Otsuki (2002), and Sabnis and Gogate (1984) were selected to validate the proposed method.

Procedure for Evaluating the Capacity of Pile Caps

The procedure for calculating the capacity of piles caps by the authors proposed method uses the compatibility, equilibrium, and constitutive relationships as described above and is as follows:

1. According to the member forces calculated from eq. [10] to eq. [12], ε_d and ε_r are found for $\boldsymbol{P}$ using eq. [13] and eq. [21], respectively. A concrete softening coefficient ξ is calculated from eq. [15] using ε_r.

2. The updated value of σ_d is calculated from eq. [13]. If the difference between the two σ_d values is larger than the defined tolerance, the steps are repeated until convergence has been achieved. Nominal strength by failure of diagonal strut can be estimated from

[22] $$P_n = 4\xi f_c' A_d \cos\theta_z$$

3. The nominal strength by failure of horizontal concrete strut is taken by

[23] $$P_n = 0.85 f_c' \frac{hc}{2} \frac{\cos\theta_z}{\cos\theta_x}$$

and, the nominal strength by tension failure mode can be expressed as

[24] $$P_n = \left(2 f_y A_s + 4F_{ct}\right)\frac{\cos\theta_z}{\cos\theta_x}$$

where f_y and A_s are the yield strength and cross-sectional area of the bottom longitudinal reinforcement. The strength of the pile cap by a tension failure mode is the column load to cause yielding of the reinforcement and fracture of a concrete tie.

4. The predicted strength by this method is the minimum value of the nominal strengths computed from the different failure modes, which are crushing or splitting of the diagonal concrete strut, crushing of the compression zone at the base of the column load, and yielding of longitudinal reinforcement.

Strength prediction

The calculated strengths by the 6 methods (special provisions for slabs and footings of ACI 318-99 and in CRSI Design Handbook 2002, and the strut-and-tie methods in ACI 318-05, CSA A23.3, by Adebar and Zhou, and by the Authors) are compared with the measured capacity of the 116 selected pile caps test results. The details of the test specimens and strength ratios (P_{test}/P_n) are presented for each of the 6 groups of test results in Tables 1-6, and collectively in Table 8 and Figs. 2-3. In all figures, the shear span a is defined by the distance from pile centre-line to column centre-line measured parallel to pile cap side. Table 7 shows the specimens which were reported to have failed by shear. Some of specimens do not satisfy the code minimum depth of 305 mm for footings on piles and the code minimum percentage of longitudinal reinforcement. Especially, the overall height of the specimens of Sabnis and Gogate (1984) is 152 mm which is about a half of code minimum footing depth, and 18 specimens of Suzuki, Otsuki, and Tsubata (1999) are tapered pile caps. However, the comparative evaluation still used this test data for the purpose of comparing the different design approaches. Tapered pile caps can be designed using strut-and-tie model as long as the inclination of tapered pile cap is small enough to include sufficient concrete area for the diagonal struts.

Fig. 2 presents the strength ratios (P_{test}/P_n) as a function of shear span-to-depth ratio for the six aforementioned methods: (a) Special provisions for slabs and footings of ACI 318-99 Code; (b) CRSI Design Handbook 2002; (c) Strut-and-tie model of ACI 318-05; (d) Strut-and-tie model of CSA A23.3; (e) Strut-and-tie model approach of Adebar and Zhou; and (f) Proposed strut-and-tie model approach by the authors. Based on these comparisons, the following initial observations can be made. The special provisions in ACI 318-99 and the design formula of CRSI Design Handbook 2002 lead to the most conservative estimates of strength with very reasonable coefficients of variation for the range of tested pile caps. The strengths calculated by the strut-and-tie provisions in Appendix A of ACI 318-05 and CSA A23.3 provide conservative estimates of capacities and somewhat larger scatter of strength ratios. The methods presented by Adebar and Zhou (1996) and the authors are less conservative, but still safe, with a scatter similar to that by the ACI and CSRI special provisions for footings and slabs.

The above observations were referred to as initial observations for a more complete examination of the behavior of the tested pile caps leads to a somewhat different assessment of the accuracy and safety of these methods. The source of the conservatism of the first four methods is that the calculated strengths, P_n, was usually controlled by the calculated flexural capacity of the test structures. These calculated capacities have been observed to be unduly conservative due to inaccuracies in the estimated flexural lever arm and ignoring tensile contributions of the concrete. Therefore, in order to evaluate the shear provisions and the strut and nodal zone stress limits of these methods, it is useful to examine the strength ratios for members that did not fail by reinforcement yielding and in which the calculated strengths are not limited by the calculated flexural capacity or strength of the tension ties.

Fig. 3 presents the strength ratios (P_{test}/P_n) as a function of shear span-to-depth ratio for the six aforementioned methods for only those 33 pile caps that were reported by the authors to have failed in shear and before reinforcement yielding and in which the nominal strength, P_n, is controlled by the calculated shear strength or strength of struts and nodes. As shown in Fig. 3, this leads to a very different impression of the accuracy and safety of these methods. The calculated shear capacities by ACI 318-99 (Fig. 3a) and CSRI (Fig. 3b) were unconservative in 17 and 19 of the 33 cases, respectively. The strut and tie provisions by ACI 318-05 (Fig. 3c) and the CSA A23.3 (Fig. 3d) were unconservative in 5 and 12 of the 33 cases, respectively. Thus, it can be concluded that while these four methods are conservative due to their underprediction of flexural and tie capacities, that the shear, concrete strut, and nodal zone capacities predicted by these methods are unconservative.

Fig. 3(e) examines the accuracy of the strut-and-tie model approach proposed by Adebar and Zhou (1996). The shear capacity predicted by this method is limited by the nodal zone bearing stresses given by eq. [2], while the flexural capacity can be described by the column load that would cause yielding of the steel tie of the strut-and-tie model. Adebar and Zhou (1996) assumed that the lower nodes of strut-and-tie model were located at the center of the piles at the level of the longitudinal reinforcement, while the upper nodal zones were assumed to be at the top surface of the pile cap. This method does not overpredict any of the pile cap strengths and the predictions are reasonably conservative as the strength of most pile caps was limited by the conservative method for calculating the flexural capacity. However, the bearing capacity requirement provides unconservative estimations of the strengths for many specimens which were reported to have failed by shear as shown in Fig. 3(e). The shear span-to-depth ratios of most test specimens reviewed in this study is less than one, and the majority of the specimens may be more accurately described as combined bending and shear failure due to interpretation of failure modes. The nodal zone bearing stress limit calculated in eq. [2] results in similar maximum bearing strengths as calculated in the ACI Code in which the stress limit is $\phi(0.85 f_c')\sqrt{A_2/A_1}$. Fig. 3(e) illustrates that the bearing strength limit of this method is not a good indicator for pile cap strengths as has been reported by Cavers and Fenton (2004).

Figs. 2(f) and 3(f) examine the accuracy of the procedure developed by the authors. The calculated capacities by the proposed method are both accurate and conservative with limited scatter or trends for pile caps with shear span-to-depth ratios ranging from 0.49 to 1.8 and concrete strength less than 41 MPa. The proposed method also provides reasonably conservative strength predictions for all the specimens that were reported to have failed in shear.

CONCLUSIONS

In this paper, a three-dimensional strut-and-tie model approach has been presented for calculating the load-carrying capacity of pile caps. The failure strength predictions for 116 tested pile caps by this method are compared with those of six methods

1. The special provisions for slabs and footings of ACI 318-99 and the CSRI methods provided the most conservative strength predictions. This conservatism is due to the particularly low estimates of flexural capacity by these methods. If the shear provisions of these methods are used to predict the capacity of those members that are reported to have failed in shear, then these shear provisions are found to be quite unconservative; the capacity of more than one-half of the tested shear-critical pile caps are over predicted.

2. The strut-and-tie model approaches in Appendix A of ACI 318-05 and the CSA A23.3 did not overpredict the measured strengths of any of the pile caps. However, the provisions of these methods for calculating the strength of struts and nodes by these methods were found to be

somewhat unconservative for those members that did not fail by reinforcement yielding.

3. The strut-and-tie approach by Adebar and Zhou did not overpredict the strength of any of the pile caps that failed by yielding of the longitudinal reinforcement and these strength predictions were reasonably accurate. However, this approach provided somewhat unconservative estimations of the shear strengths for many of the test specimens that were reported to have failed by shear.

4. The calculated capacities by the proposed method were both accurate and conservative with little scatter or trends for tested pile caps with shear span-to-depth ratios ranging from 0.49 to 1.8 and concrete strength less than 41 MPa. The success of the proposed method indicates that a strut-and-tie design philosophy is appropriate for the design of pile caps.

List of symbols:

$a\ d, h$ — the distance from pile centre-line to column center-line measured parallel to pile cap side, effective depth, overall height

A_d, A_{ct} — effective areas of diagonal strut and concrete tie

A_s — cross-sectional area of main reinforcement

b_o — perimeter of critical section

c, d_p, l_e — column size, pile diameter, pile spacing

f_c' — compressive strength of concrete cylinder

f_{cr} — concrete tensile strength

f_{ct} — tensile stress of concrete tie

f_{cu} — effective strength of concrete strut

f_y — yield strength of reinforcement

F_{ct} — nominal strength of concrete tie

F_d, F_x, F_y — the forces of diagonal, x, and y-directional members

w — distance between column face and center line of pile

$\theta_x, \theta_y, \theta_z$ — inclination angle between diagonal strut and x, y, and z-axis

θ_s — inclination angel between diagonal strut and steel tie

w_c, w_d — effective width of horizontal strut and diagonal strut

σ_d — compressive stress of concrete strut

ε_0 — strain at peak stress of standard cylinder

ε_s — tensile strain of steel tie

$\varepsilon_h, \varepsilon_v$ — strain of horizontal direction and vertical direction

ε_d compressive strain of diagonal strut

ε_r tensile strain of the direction perpendicular to diagonal strut

References:

ACI Committee 318. 1999. Building code requirements for reinforced concrete (ACI 318-99) and commentary (ACI 318R-99). American Concrete Institute.

ACI Committee 318. 2002. Building code requirements for reinforced concrete (ACI 318-02) and commentary (ACI 318R-02). American Concrete Institute.

ACI Committee 318. 2005. Building code requirements for reinforced concrete (ACI 318-05) and commentary (ACI 318R-05). American Concrete Institute.

CSA Committee A23.3. 1984. Design of concrete structures for buildings. Standard A23.3-M84, Canadian Standards Association.

CSA Committee A23.3. 2004. Design of concrete structures for buildings. Standard A23.3-M04, Canadian Standards Association.

AASHTO. 1994. AASHTO LRFD bridge design specifications, American Association of State Highway Transportation Officials.

Schlaich, J., Schäfer, K., and Jennewein, M. 1987. Toward a consistent design of reinforced structural concrete. Journal of Prestressed Concrete Institute, **32**(3): 74-150.

Adebar, P., and Zhou, Z. 1993. Bearing strength of compressive struts confined by plain concrete. ACI Structural Journal, **90**(5): 534-541.

Adebar, P., and Zhou, Z. 1996. Design of deep pile caps by strut-and-tie models. ACI Structural Journal, **93**(4): 437-448.

CRSI. 2002. CRSI Design Handbook, Concrete Reinforcing Steel Institute.

Martinez, S., NiIson, A. H., and Slate, F. O. 1982. Spirally-reinforced high-strength concrete columns. Research Report No. 82-10, Department of Structural Engineering, Cornell University, Ithaca.

Paulay, T., and Priestley, M. J. N. 1992. Seismic design of reinforced concrete and masonry buildings, John Wiley and Sons.

Hsu, T. T. C., and Zhang, L. X. B. 1997. Nonlinear analysis of membrane elements by fixed-angle softened-truss model. ACI Structural Journal, **94**(5): 483-492.

Foster, S. J., and Gilbert, R. I. 1996. The design of nonflexural members with normal and high-strength concretes. ACI Structural Journal, **93**(1): 3-10.

Vecchio, F. J., and Collins, M. P. 1986. Modified compression field theory for reinforced concrete elements subjected to shear. ACI Journal, **83**(2): 219-231.

Blévot, J., and Frémy, R. 1967. Semelles sur Pieux," Annales de l'Institut Technique du Batiment et des Travaux Publics, **20**(230): 223-295.

Clarke, J. L. 1973. Behavior and design of pile caps with four piles. Cement and Concrete Association, Report No. 42.489, London.

Sabnis, G. M., and Gogate, A. B. 1984. Investigation of thick slab (pile cap) behavior. ACI Journal, **81**(1): 35-39.

Adebar, P., Kuchma, D., and Collins, M. P. 1990. Strut-and-tie models for the design of pile caps: An experimental study. ACI Structural Journal, **87**(1): 81-92.

Suzuki, K., Otsuki, K., and Tsubata, T. 1998. Influence of bar arrangement on ultimate strength of four-pile caps. Transactions of the Japan Concrete Institute, **20**: 195–202.

Suzuki, K., Otsuki, K., and Tsubata, T. 1999. Experimental study on four-pile caps with taper. Transactions of the Japan Concrete Institute, **21**: 327-334.

Suzuki, K., Otsuki, K., and Tsuchiya, T. 2000. Influence of edge distance on failure mechanism of pile caps. Transactions of the Japan Concrete Institute, **22**: 361-368.

Suzuki, K., and Otsuki, K. 2002. Experimental study on corner shear failure of pile caps. Transactions of the Japan Concrete Institute, **23**: 303-310.

Bloodworth, A. G., Jackson, P. A., and Lee, M. M. K. 2003. Strength of reinforced concrete pile caps. Proceedings of the Institution of Civil Engineers, Structures & Buildings, **156**: 347–358.

Cavers, W., and Fenton, G. A. 2004. An evaluation of pile cap design methods in accordance with the Canadian design standard. Canadian Journal of Civil Engineering, **31**: 109-119.

Vecchio, F. J., and Collins, M. P. 1982. Response of reinforced concrete to in-plane shear and normal stresses. Report No. 82-03, University of Toronto, Toronto, Canada.

Vecchio, F. J., and Collins, M. P. 1993. Compression response of cracked reinforced concrete. ASCE, Journal of Structural Engineering, **119**(12): 3590-3610.

Park, J. W., and Kuchma, D. 2006. Strut-and-tie model analysis for strength prediction of deep beams. ACI Structural Journal, Submitted.

Table captions:

Table 1 – Test data of Clarke (1973)

Table 2 – Test data of Suzuki, Otsuki, and Tsubata (1998)

Table 3 – Test data of Suzuki, Otsuki, and Tsubata (1999)

Table 4 – Test data of Suzuki, Otsuki, and Tsuchiya (2000)

Table 5 – Test data of Suzuki, and Otsuki (2002)

Table 6 – Test data of Sabnis and Gogate (1984)

Table 7 – Test specimens reported to have failed by shear

Table 8 – Ratio of measured to predicted strength

Figure captions:

Fig. 1 – A strut-and-tie model for pile caps

Fig. 2 – Ratio of measured to predicted strength with respect to shear span-depth ratio: (a) Special provisions for slabs and footings of ACI 318-99; (b) CRSI Design Handbook 2002; (c) Strut-and-tie model of ACI 318-05; (d) Strut-and-tie model of CSA A23.3; (e) Strut-and-tie model approach of Adebar and Zhou; (f) Proposed strut-and-tie model approach

Fig. 3 – Ratio of measured to calculated strengths by shear failure mode with respect to shear span-depth ratio: (a) Special provisions for slabs and footings of ACI 318-99; (b) CRSI Design Handbook 2002; (c) Strut-and-tie model of ACI 318-05; (d) Strut-and-tie model of CSA A23.3; (e) Strut-and-tie model approach of Adebar and Zhou; (f) Proposed strut-and-tie model approach

Table 1 – Test data of Clarke (1973)

pile cap	f'_c (MPa)	cap size (mm×mm)	l_e (mm)	(a)	bar arrangement
A1	21.3	950×950	600	10	grid
A2	27.2	950×950	600	10	bunched
A4	21.4	950×950	600	10	grid
A5	26.6	950×950	600	10	bunched
A7	24.2	950×950	600	10	grid
A8	27.2	950×950	600	10	bunched
A9	26.6	950×950	600	10	grid
A10	18.8	950×950	600	10	grid
A11	18.0	950×950	600	10	grid
A12	25.3	950×950	600	10	grid
B1	26.7	750×750	400	8	grid
B2	24.5	750×750	400	10	grid
B3	35.0	750×750	400	6	grid

Note: (a) number of D10 bars at both of x and y direction; pile spacing l_e; yield strength of reinforcement f_y =410 MPa, overall height h =450 mm, effective depth d =405 mm, column width c =200 mm, pile diameter d_p =200 mm for all specimens

Table 2 – Test data of Suzuki, Otsuki, and Tsubata (1998)

pile cap	f'_c (MPa)	cap size (mm×mm)	l_e (mm)	h (mm)	d (mm)	c (mm)	(a)	f_y (MPa)		bar arrangement
								x-dir.	y-dir.	
BP-20-1	21.3	900×900	540	200	150	300	8	413	413	grid
BP-20-2	20.4	900×900	540	200	150	300	8	413	413	grid
BPC-20-1	21.9	900×900	540	200	150	300	8	413	413	bunched
BPC-20-2	19.9	900×900	540	200	150	300	8	413	413	bunched
BP-25-1	22.6	900×900	540	250	200	300	10	413	413	grid
BP-25-2	21.5	900×900	540	250	200	300	10	413	413	grid
BPC-25-1	18.9	900×900	540	250	200	300	10	413	413	bunched
BPC-25-2	22.0	900×900	540	250	200	300	10	413	413	bunched
BP-20-30-1	29.1	800×800	500	200	150	300	6	405	405	grid
BP-20-30-2	29.8	800×800	500	200	150	300	6	405	405	grid
BPC-20-30-1	29.8	800×800	500	200	150	300	6	405	405	bunched
BPC-20-30-2	29.8	800×800	500	200	150	300	6	405	405	bunched
BP-30-30-1	27.3	800×800	500	300	250	300	8	405	405	grid
BP-30-30-2	28.5	800×800	500	300	250	300	8	405	405	grid
BPC-30-30-1	28.9	800×800	500	300	250	300	8	405	405	bunched
BPC-30-30-2	30.9	800×800	500	300	250	300	8	405	405	bunched
BP-30-25-1	30.9	800×800	500	300	250	250	8	405	405	grid
BP-30-25-2	26.3	800×800	500	300	250	250	8	405	405	grid
BPC-30-25-1	29.1	800×800	500	300	250	250	8	405	405	bunched
BPC-30-25-2	29.2	800×800	500	300	250	250	8	405	405	bunched
BDA-70-90-1	29.1	700×900	500	300	250	250	8	356	345	grid
BDA-70-90-2	30.2	700×900	500	300	250	250	8	356	345	grid
BDA-80-90-1	29.1	800×900	500	300	250	250	8	356	345	grid
BDA-80-90-2	29.3	800×900	500	300	250	250	8	356	345	grid
BDA-90-90-1	29.5	900×900	500	300	250	250	8	356	345	grid
BDA-90-90-2	31.5	900×900	500	300	250	250	8	356	345	grid
BDA-100-90-1	29.7	1000×900	500	300	250	250	8	356	345	grid
BDA-100-90-2	31.3	1000×900	500	300	250	250	8	356	345	grid

Note: (a) number of D10 bars at both of x and y direction; pile diameter d_p =150 mm for all specimens

Table 3 – Test data of Suzuki, Otsuki, and Tsubata (1999)

pile cap	f_c' (MPa)	l_e (mm)	h (mm)	d (mm)	(a)	(b)
TDL1-1	30.9	600	350	300	4	356
TDL1-2	28.2	600	350	300	4	356
TDL2-1	28.6	600	350	300	6	356
TDL2-2	28.8	600	350	300	6	356
TDL3-1	29.6	600	350	300	8	356
TDL3-2	29.3	600	350	300	8	356
TDS1-1	25.6	450	350	300	6	356
TDS1-2	27.0	450	350	300	6	356
TDS2-1	27.2	450	350	300	8	356
TDS2-2	27.3	450	350	300	8	356
TDS3-1	28.0	450	350	300	11	356
TDS3-2	28.1	450	350	300	11	356
TDM1-1	27.5	500	300	250	4	383
TDM1-2	26.3	500	300	250	4	383
TDM2-1	29.6	500	300	250	6	383
TDM2-2	27.6	500	300	250	6	383
TDM3-1	27.0	500	300	250	10	370
TDM3-2	28.0	500	300	250	10	370

Note: (a) number of D10 bars at both of x and y direction; (b) yield strength of reinforcement at both of x and y direction in MPa; pile cap size 900×900 mm, column width c =250 mm, pile diameter d_p =150 mm, grid type of bar arrangement for all specimens

Table 4 – Test data of Suzuki, Otsuki, and Tsuchiya (2000)

pile cap	f_c' (MPa)	cap size (mm×mm)	h (mm)	d (mm)	c (mm)	(a)	(b)
BDA-20-25-70-1	26.1	700×700	200	150	250	4	358
BDA-20-25-70-2	26.1	700×700	200	150	250	4	358
BDA-20-25-80-1	25.4	800×800	200	150	250	4	358
BDA-20-25-80-2	25.4	800×800	200	150	250	4	358
BDA-20-25-90-1	25.8	900×900	200	150	250	4	358
BDA-20-25-90-2	25.8	900×900	200	150	250	4	358
BDA-30-20-70-1	25.2	700×700	300	250	200	6	358
BDA-30-20-70-2	24.6	700×700	300	250	200	6	358
BDA-30-20-80-1	25.2	800×800	300	250	200	6	358
BDA-30-20-80-2	26.6	800×800	300	250	200	6	358
BDA-30-20-90-1	26.0	900×900	300	250	200	6	358
BDA-30-20-90-2	26.1	900×900	300	250	200	6	358
BDA-30-25-70-1	28.8	700×700	300	250	250	6	383
BDA-30-25-70-2	26.5	700×700	300	250	250	6	383
BDA-30-25-80-1	29.4	800×800	300	250	250	6	383
BDA-30-25-80-2	27.8	800×800	300	250	250	6	383
BDA-30-25-90-1	29.0	900×900	300	250	250	6	383
BDA-30-25-90-2	26.8	900×900	300	250	250	6	383
BDA-30-30-70-1	26.8	700×700	300	250	300	6	358
BDA-30-30-70-2	25.9	700×700	300	250	300	6	358
BDA-30-30-80-1	27.4	800×800	300	250	300	6	358
BDA-30-30-80-2	27.4	800×800	300	250	300	6	358
BDA-30-30-90-1	27.2	900×900	300	250	300	6	358
BDA-30-30-90-2	24.5	900×900	300	250	300	6	358
BDA-40-25-70-1	25.9	700×700	400	350	250	8	358
BDA-40-25-70-2	24.8	700×700	400	350	250	8	358
BDA-40-25-80-1	26.5	800×800	400	350	250	8	358
BDA-40-25-80-2	25.5	800×800	400	350	250	8	358
BDA-40-25-90-1	25.7	900×900	400	350	250	8	358
BDA-40-25-90-2	26.0	900×900	400	350	250	8	358

Note: (a) number of D10 bars at both of x and y direction; (b) yield strength of reinforcement at both of x and y direction in MPa; pile spacing l_e =450 mm, pile diameter d_p =150 mm, grid type of bar arrangement for all specimens

Table 5 – Test data of Suzuki, and Otsuki (2002)

pile cap	f_c' (MPa)	c (mm)	anchorage
BPL-35-30-1	24.1	300	180-deg. hook
BPL-35-30-2	25.6	300	180-deg. hook
BPB-35-30-1	23.7	300	bent-up
BPB-35-30-2	23.5	300	bent-up
BPH-35-30-1	31.5	300	180-deg. hook
BPH-35-30-2	32.7	300	180-deg. hook
BPL-35-25-1	27.1	250	180-deg. hook
BPL-35-25-2	25.6	250	180-deg. hook
BPB-35-25-1	23.2	250	bent-up
BPB-35-25-2	23.7	250	bent-up
BPH-35-25-1	36.6	250	180-deg. hook
BPH-35-25-2	37.9	250	180-deg. hook
BPL-35-20-1	22.5	200	180-deg. hook
BPL-35-20-2	21.5	200	180-deg. hook
BPB-35-20-1	20.4	200	bent-up
BPB-35-20-2	20.2	200	bent-up
BPH-35-20-1	31.4	200	180-deg. hook
BPH-35-20-2	30.8	200	180-deg. hook

Note: 9-D10 bars at both of x and y direction; yield strength of reinforcement f_y =353 MPa; pile cap size 800×800 mm, pile spacing l_e =500 mm, overall height h =350 mm, effective depth d =300 mm, pile diameter d_p =150 mm, grid type of bar arrangement for all specimens

Table 6 – Test data of Sabnis and Gogate (1984)

pile cap	f_c' (MPa)	d (mm)	(a)	(b)
SS1	31.3	111	0.0021	499
SS2	31.3	112	0.0014	662
SS3	31.3	111	0.00177	886
SS4	31.3	112	0.0026	482
SS5	41.0	109	0.0054	498
SS6	41.0	109	0.0079	499
SG1	17.9	152	0	-
SG2	17.9	117	0.0055	414
SG3	17.9	117	0.0133	414

Note: (a) reinforcement ratio at both of x and y direction; (b) yield strength of reinforcement at both of x and y direction in MPa; pile cap size 330×330 mm, pile spacing l_e =203 mm, overall height h =152 mm, column diameter c =76 mm, pile diameter d_p =76 mm, grid type of bar arrangement for all specimens

Table 7 – Test specimens reported to have failed by shear

Author	pile cap specimens
Clarke (1973)	A1, A2, A4, A5, A7, A8, A9, A10
Suzuki, Otsuki, and Tsubata (1998)	BP-25-1, BP-25-2, BP-30-30-1, BP-30-25-2
Suzuki, Otsuki, and Tsubata (1999)	BDA-40-25-70-1
Suzuki, Otsuki, and Tsuchiya (2000)	TDM3-1, TDM3-2
Suzuki, and Otsuki (2002)	BPL-35-30-1, BPL-35-30-2, BPH-35-30-1, BPL-35-25-2, BPH-35-25-1, BPH-35-25-2, BPL-35-20-1, BPL-35-20-2, BPH-35-20-1, BPH-35-20-2
Sabnis and Gogate (1984)	SS1, SS2, SS3, SS4, SS5, SS6, SG2, SG3

Table 8 – Ratio of measured to predicted strength

specimen	P_{test} (kN)	P_{test}/P_n (a)	(b)	(c)	(d)	(e)	(f)
BP-20-1	519	2.08	2.08	1.69	1.80	1.43	1.51
BP-20-2	480	1.93	1.93	1.57	1.67	1.32	1.45
BPC-20-1	519	2.08	2.08	1.69	1.80	1.43	1.48
BPC-20-2	529	2.13	2.13	1.73	1.84	1.46	1.64
BP-25-1	735	1.76	1.76	1.52	1.46	1.22	1.51
BP-25-2	755	1.81	1.81	1.64	1.51	1.25	1.63
BPC-25-1	818	1.98	1.98	2.02	1.64	1.35	2.01
BPC-25-2	813	1.95	1.95	1.73	1.62	1.35	1.72
BP-20-30-1	485	2.40	2.40	1.93	2.02	1.63	1.62
BP-20-30-2	480	2.38	2.38	1.91	2.00	1.62	1.60
BPC-20-30-1	500	2.48	2.48	1.99	2.08	1.68	1.67
BPC-20-30-2	495	2.45	2.45	1.97	2.06	1.67	1.65
BP-30-30-1	916	2.03	2.03	1.52	1.58	1.39	1.34
BP-30-30-2	907	2.01	2.01	1.50	1.57	1.37	1.32
BPC-30-30-1	1039	2.30	2.30	1.72	1.79	1.57	1.51
BPC-30-30-2	1029	2.28	2.28	1.71	1.77	1.56	1.49
BP-30-25-1	794	1.76	1.76	1.44	1.51	1.29	1.23
BP-30-25-2	725	1.61	1.61	1.32	1.39	1.18	1.14
BPC-30-25-1	853	1.89	1.89	1.55	1.62	1.38	1.33
BPC-30-25-2	872	1.93	1.93	1.58	1.66	1.42	1.36
BDA-70-90-1	784	1.97	1.97	1.62	1.70	1.45	1.36
BDA-70-90-2	755	1.89	1.89	1.56	1.63	1.39	1.30
BDA-80-90-1	858	2.15	2.15	1.77	1.86	1.58	1.49
BDA-80-90-2	853	2.14	2.14	1.76	1.85	1.58	1.48
BDA-90-90-1	853	2.14	2.14	1.76	1.84	1.58	1.48
BDA-90-90-2	921	2.31	2.31	1.90	1.99	1.70	1.59
BDA-100-90-1	911	2.28	2.28	1.88	1.97	1.68	1.58
BDA-100-90-2	931	2.33	2.33	1.92	2.01	1.72	1.60
A1	1110	1.44	1.44	1.73	1.53	1.17	1.10
A2	1420	1.83	1.83	1.73	1.74	1.50	1.33
A4	1230	1.59	1.59	1.91	1.69	1.30	1.22
A5	1400	1.80	1.80	1.75	1.72	1.48	1.31
A7	1640	2.12	2.12	2.25	2.03	1.73	1.55
A8	1510	1.95	1.95	1.84	1.85	1.59	1.41
A9	1450	1.87	1.87	1.81	1.78	1.53	1.36
A10	1520	1.97	1.97	2.68	2.38	1.60	1.71
A11	1640	2.13	2.13	3.02	2.68	1.73	1.92
A12	1640	2.12	2.12	2.15	2.02	1.73	1.55
B1	2080	2.23	2.23	2.29	2.29	1.65	1.79
B2	1900	1.64	1.64	2.28	2.28	1.20	1.78
B3	1770	2.52	2.52	1.97	2.06	1.87	1.50
BPL-35-30-1	960	1.81	1.81	1.32	1.38	1.24	1.26
BPL-35-30-2	941	1.77	1.77	1.30	1.35	1.21	1.18
BPB-35-30-1	1029	1.94	1.94	1.42	1.48	1.32	1.38
BPB-35-30-2	1103	2.08	2.08	1.52	1.59	1.42	1.49
BPH-35-30-1	980	1.83	1.83	1.35	1.40	1.26	1.16
BPH-35-30-2	1088	2.04	2.04	1.50	1.55	1.40	1.28
BPL-35-25-1	902	1.69	1.69	1.36	1.42	1.24	1.16
BPL-35-25-2	872	1.64	1.64	1.31	1.38	1.20	1.13
BPB-35-25-1	911	1.72	1.72	1.37	1.45	1.26	1.30
BPB-35-25-2	921	1.73	1.73	1.38	1.46	1.27	1.29
BPH-35-25-1	882	1.65	1.65	1.33	1.38	1.22	1.10
BPH-35-25-2	951	1.78	1.78	1.43	1.49	1.31	1.18
BPL-35-20-1	755	1.42	1.42	1.24	1.33	1.11	1.15
BPL-35-20-2	735	1.39	1.39	1.21	1.30	1.08	1.17
BPB-35-20-1	755	1.43	1.43	1.31	1.34	1.11	1.27
BPB-35-20-2	804	1.52	1.52	1.41	1.43	1.18	1.37
BPH-35-20-1	813	1.52	1.52	1.33	1.41	1.20	1.10
BPH-35-20-2	794	1.49	1.49	1.30	1.38	1.17	1.08

specimen	P_{test} (kN)	P_{test}/P_n (a)	(b)	(c)	(d)	(e)	(f)
BDA-20-25-70-1	294	2.22	2.22	1.93	2.03	1.57	1.46
BDA-20-25-70-2	304	2.29	2.29	1.99	2.10	1.62	1.51
BDA-20-25-80-1	304	2.29	2.29	1.99	2.10	1.62	1.51
BDA-20-25-80-2	304	2.29	2.29	1.99	2.10	1.62	1.51
BDA-20-25-90-1	333	2.50	2.50	2.18	2.30	1.77	1.65
BDA-20-25-90-2	333	2.50	2.50	2.18	2.30	1.77	1.65
BDA-30-20-70-1	534	1.61	1.61	1.40	1.50	1.23	1.12
BDA-30-20-70-2	549	1.65	1.65	1.44	1.54	1.26	1.16
BDA-30-20-80-1	568	1.71	1.71	1.49	1.60	1.30	1.19
BDA-30-20-80-2	564	1.69	1.69	1.48	1.58	1.29	1.18
BDA-30-20-90-1	583	1.75	1.75	1.53	1.64	1.34	1.22
BDA-30-20-90-2	588	1.76	1.76	1.54	1.65	1.35	1.23
BDA-30-25-70-1	662	1.86	1.86	1.47	1.54	1.32	1.21
BDA-30-25-70-2	676	1.90	1.90	1.50	1.57	1.35	1.24
BDA-30-25-80-1	696	1.95	1.95	1.54	1.62	1.39	1.27
BDA-30-25-80-2	725	2.03	2.03	1.61	1.69	1.44	1.33
BDA-30-25-90-1	764	2.14	2.14	1.69	1.78	1.52	1.39
BDA-30-25-90-2	764	2.14	2.14	1.69	1.78	1.52	1.40
BDA-30-30-70-1	769	2.31	2.31	1.64	1.72	1.51	1.38
BDA-30-30-70-2	730	2.20	2.20	1.56	1.63	1.44	1.31
BDA-30-30-80-1	828	2.48	2.48	1.77	1.85	1.63	1.48
BDA-30-30-80-2	809	2.43	2.43	1.73	1.81	1.59	1.44
BDA-30-30-90-1	843	2.52	2.52	1.80	1.88	1.66	1.51
BDA-30-30-90-2	813	2.44	2.44	1.74	1.81	1.60	1.47
BDA-40-25-70-1	1019	1.64	1.64	1.24	1.29	1.16	1.12
BDA-40-25-70-2	1068	1.72	1.72	1.30	1.35	1.22	1.23
BDA-40-25-80-1	1117	1.79	1.79	1.36	1.41	1.28	1.20
BDA-40-25-80-2	1117	1.80	1.80	1.36	1.41	1.28	1.25
BDA-40-25-90-1	1176	1.89	1.89	1.43	1.49	1.34	1.31
BDA-40-25-90-2	1181	1.89	1.89	1.43	1.49	1.35	1.30
TDL1-1	392	1.94	1.94	1.68	1.74	1.53	1.06
TDL1-2	392	1.95	1.95	1.68	1.74	1.53	1.08
TDL2-1	519	1.72	1.72	1.48	1.54	1.35	1.10
TDL2-2	472	1.57	1.57	1.35	1.40	1.23	1.00
TDL3-1	608	1.52	1.52	1.30	1.35	1.19	1.04
TDL3-2	627	1.57	1.57	1.34	1.39	1.22	1.07
TDS1-1	921	2.30	2.30	1.77	1.85	1.64	1.44
TDS1-2	833	2.08	2.08	1.60	1.67	1.48	1.29
TDS2-1	1005	1.89	1.89	1.45	1.52	1.34	1.24
TDS2-2	1054	1.98	1.98	1.52	1.59	1.41	1.30
TDS3-1	1299	1.78	1.78	1.40	1.44	1.26	1.42
TDS3-2	1303	1.79	1.79	1.40	1.45	1.26	1.42
TDM1-1	490	2.27	2.27	1.88	1.97	1.68	1.37
TDM1-2	461	2.13	2.13	1.77	1.85	1.58	1.30
TDM2-1	657	2.03	2.03	1.68	1.76	1.50	1.35
TDM2-2	657	2.04	2.04	1.68	1.76	1.50	1.36
TDM3-1	1245	1.53	1.44	1.72	1.21	0.99	1.72
TDM3-2	1210	1.46	1.38	1.61	1.17	0.97	1.63
SS1	250	3.04	3.04	2.76	2.96	2.48	2.31
SS2	245	3.40	3.40	3.07	3.23	2.78	2.52
SS3	248	2.04	2.04	2.71	2.04	1.65	1.72
SS4	226	2.32	2.32	2.42	2.29	1.89	1.81
SS5	264	1.61	1.61	2.21	1.66	1.09	1.43
SS6	280	1.71	1.71	2.34	1.76	1.16	1.52
SG1	50	-	-	-	-	-	1.53
SG2	173	1.43	1.43	3.11	2.49	1.20	1.97
SG3	177	1.46	1.46	3.20	2.55	1.23	2.01
Average		**1.97**	**1.96**	**1.73**	**1.74**	**1.44**	**1.41**
Coefficient of Variation		**0.17**	**0.17**	**0.24**	**0.20**	**0.18**	**0.18**

Note: P_{test} = measured failure load; (a) Special provisions for slabs and footings of ACI 318-99; (b) CRSI Design Handbook 2002; (c) Strut-and-tie model of ACI 318-05; (d) Strut-and-tie model of CSA A23.3; (e) Strut-and-tie model approach of Adebar and Zhou; (f) Proposed strut-and-tie model approach

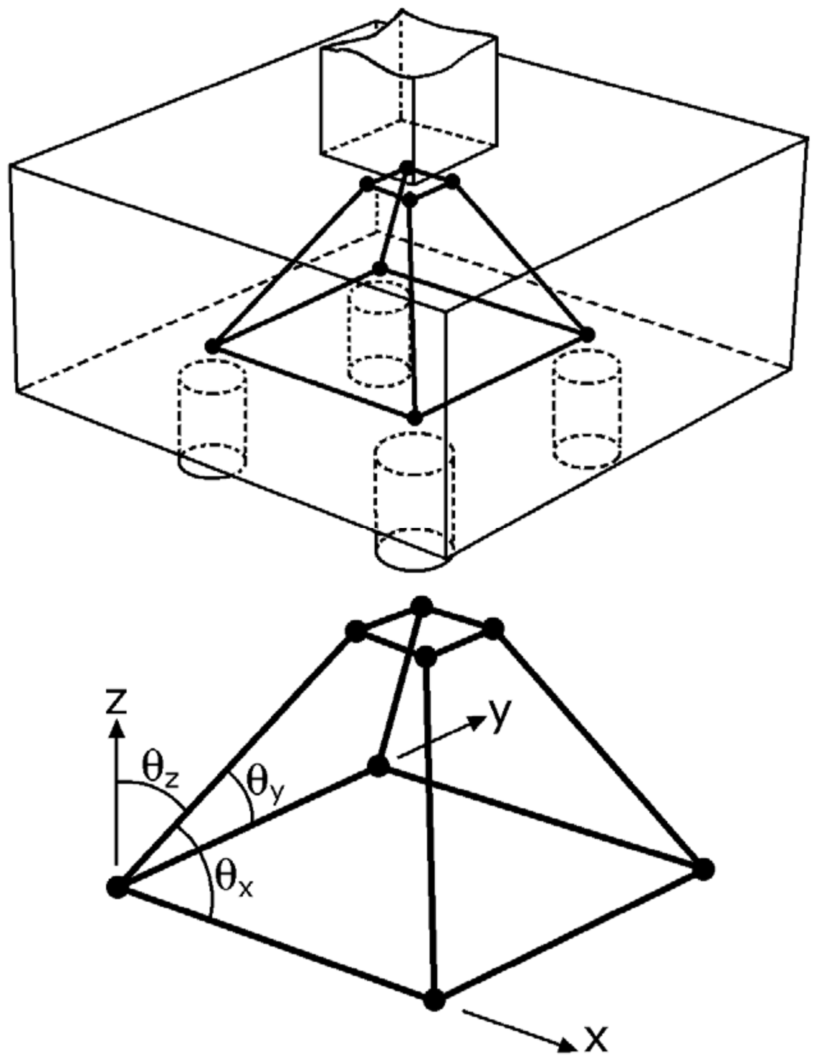

Fig. 1 – A strut-and-tie model for pile caps

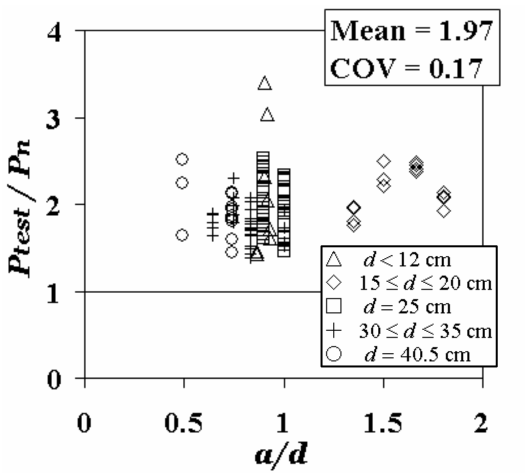
Mean = 1.97
COV = 0.17
Ptest / Pn
a/d
d < 12 cm
15 ≤ d ≤ 20 cm
d = 25 cm
30 ≤ d ≤ 35 cm
d = 40.5 cm

(a)

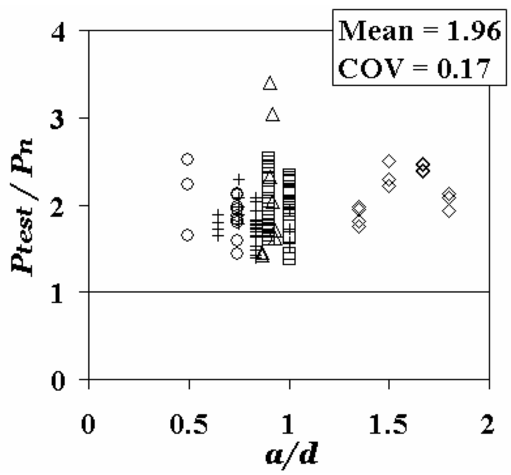
Mean = 1.96
COV = 0.17
Ptest / Pn
a/d

(b)

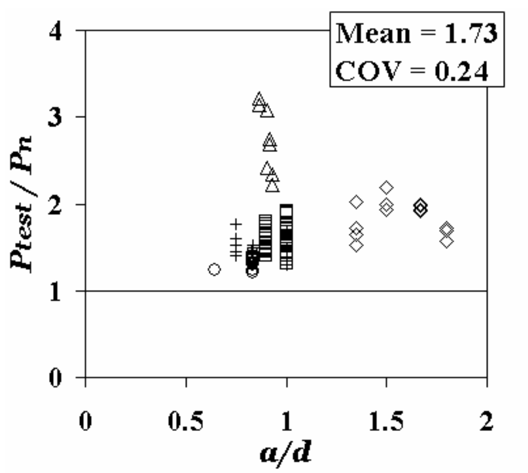
Mean = 1.73
COV = 0.24
Ptest / Pn
a/d

(c)

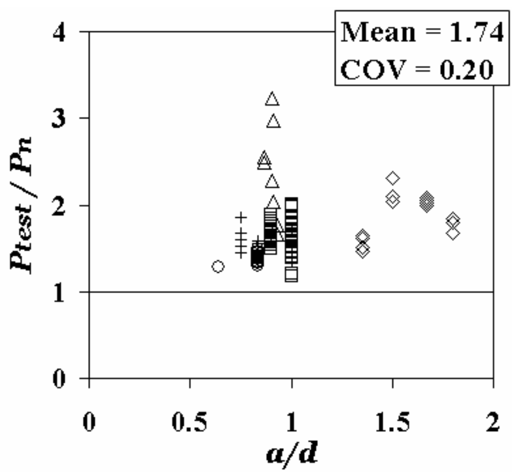
Mean = 1.74
COV = 0.20
Ptest / Pn
a/d

(d)

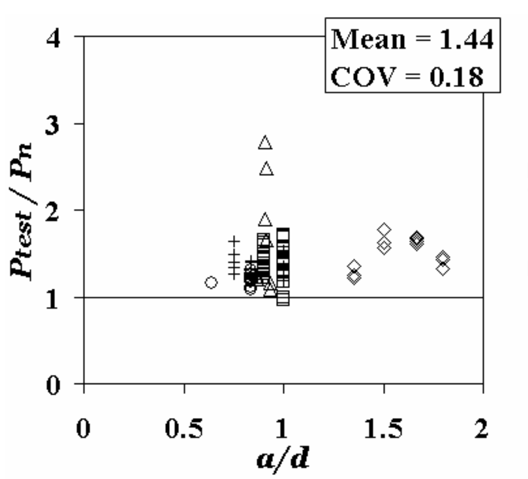
Mean = 1.44
COV = 0.18
Ptest / Pn
a/d

(e)

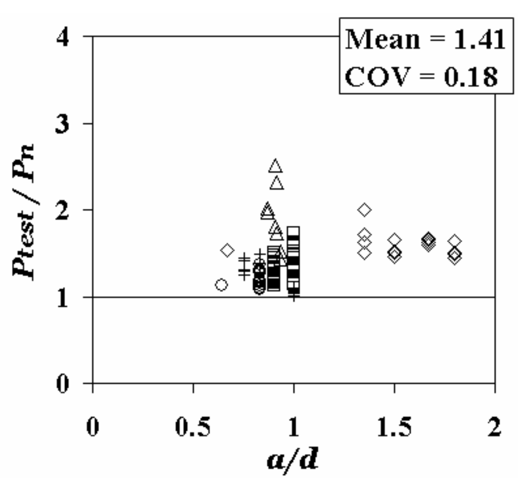
Mean = 1.41
COV = 0.18
Ptest / Pn
a/d

(f)

Fig. 2 – Ratio of measured to predicted strength with respect to shear span-depth ratio: (a) Special provisions for slabs and footings of ACI 318-99; (b) CRSI Design Handbook 2002; (c) Strut-and-tie model of ACI 318-05; (d) Strut-and-tie model of CSA A23.3; (e) Strut-and-tie model approach of Adebar and Zhou; (f) Proposed strut-and-tie model approach

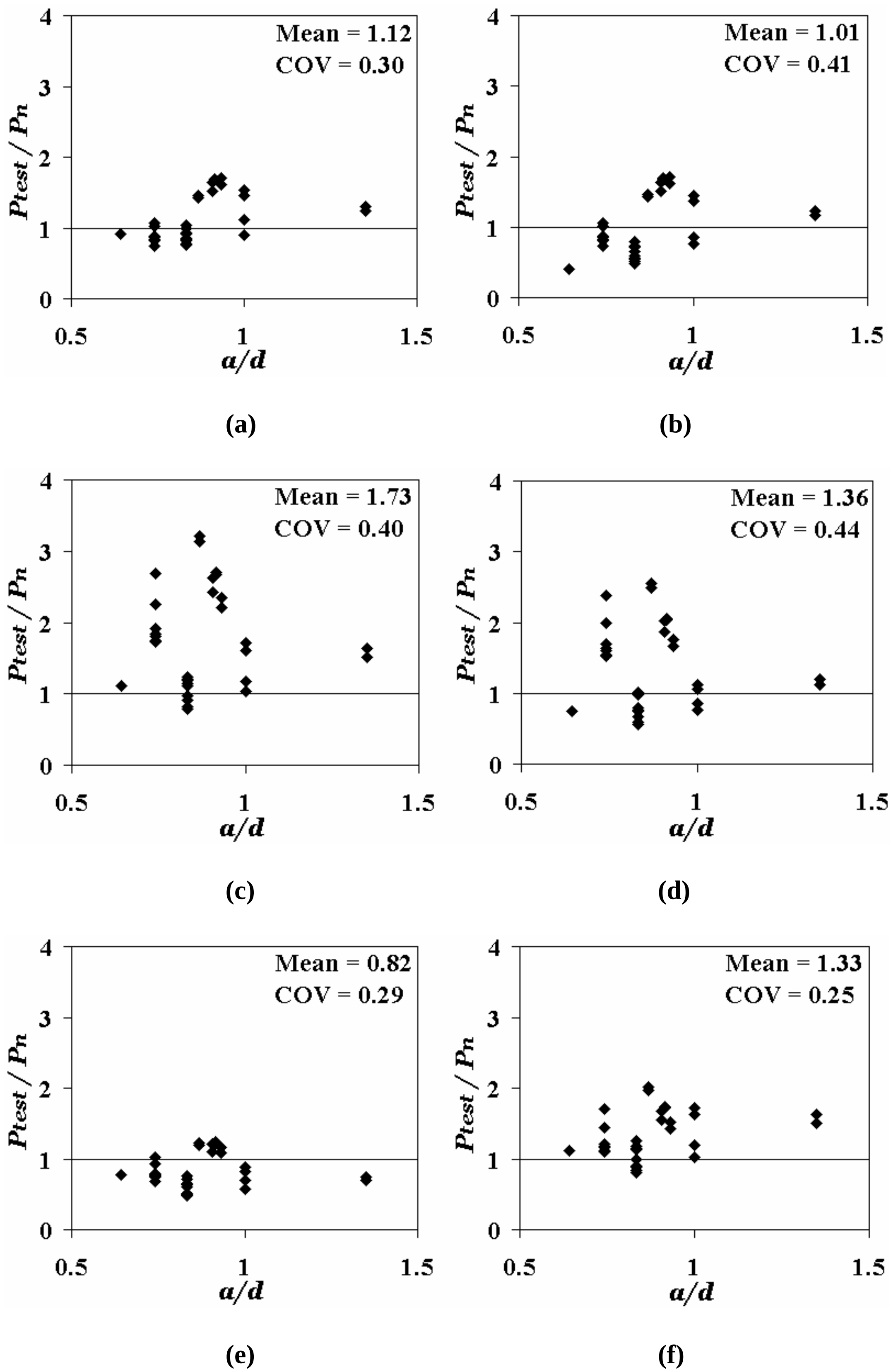

Fig. 3 – Ratio of measured to calculated shear strengths for the specimens failed by shear

with respect to shear span-depth ratio: (a) Special provisions for slabs and footings of ACI 318-99; (b) CRSI Design Handbook 2002; (c) Strut-and-tie model of ACI 318-05; (d) Strut-and-tie model of CSA A23.3; (e) Strut-and-tie model approach of Adebar and Zhou; (f) Proposed strut-and-tie model approach